

Microwave Equivalent Circuit Modeling of 29 GHz Modulated 850 nm Oxide-Confined VCSELs

Curtis Y. Wang, Michael Liu, Fei Tan and Milton Feng

Department of Electrical and Computer Engineering, University of Illinois at Urbana-Champaign
 Micro and Nanotechnology Laboratory, 208 N. Wright Street, Urbana, IL 61801
 e-mail: mfeng@illinois.edu

Keywords: Vertical Cavity Surface-Emitting Laser (VCSEL), Microwave Equivalent Circuit Modeling

Abstract

We have demonstrated a Vertical Cavity Surface Emitting Laser with modulation bandwidth, f_{-3dB} , of 29 GHz and achieved 57 Gb/s error-free ($BER \leq 10^{-12}$) data transmission at 25 °C. In this work, we have established the microwave equivalent circuit model and the data fitting technique to extract electrical parasitic parameters of the VCSEL. Ultimately we are able to extract two important parameters, namely the recombination lifetime and the photon lifetime from the measured results. We also show comparison between the overall and intrinsic optical modulation bandwidth.

INTRODUCTION

Optical links based on energy-efficient directly modulated 850 nm oxide-confined vertical cavity surface-emitting lasers and multimode optical fiber have been deployed widely in data centers for short-haul large traffic data communication. The native oxide was first invented and implemented in edge-emitting diode lasers [1] and then VCSELs [2] for electrical and optical confinement. Besides electrical carrier and optical modal confinement, the oxide apertures formed by lateral oxidation also provide scaling capability of the optical modal dimension for high speed VCSELs. Error-free data transmission higher than 40 Gb/s with 850 nm VCSELs has been demonstrated by Chalmers, TU-Berlin and UIUC [3, 4, 5]. Recently, we have demonstrated 57 Gb/s error-free data transmission and a > 29 GHz modulation bandwidth, f_{-3dB} , for a 5 μm VCSEL [6]. Previous efforts on microwave equivalent circuit modeling of VCSELs have been performed at lower speed [7, 8]. This microwave technique can be applied to higher bandwidth VCSELs to realize the intrinsic optical modulation bandwidth and to determine the intrinsic photon and recombination lifetimes by calibrating out the effect of photodetector and de-embedding the input parasitic effect [7].

In this work, we have developed a microwave equivalent circuit model on our 29 GHz bandwidth oxide-confined VCSEL with 57 Gb/s error free data transmission to extract electrical parasitic parameters and the

recombination and photon lifetimes via de-embedding bias dependent transfer functions obtained from optical bandwidth measurement and photodetector calibration.

EQUIVALENT CIRCUIT MODELING AND ELECTRICAL PARASITIC PARAMETERS EXTRACTION

Previously, we have shown a schematic of microcavity VCSEL to model the electrical parasitic parameters [7]. A modified version of the schematic for our newly designed epitaxy, layer structure and fabrication steps described in Ref. [6], is shown in Figure 1.

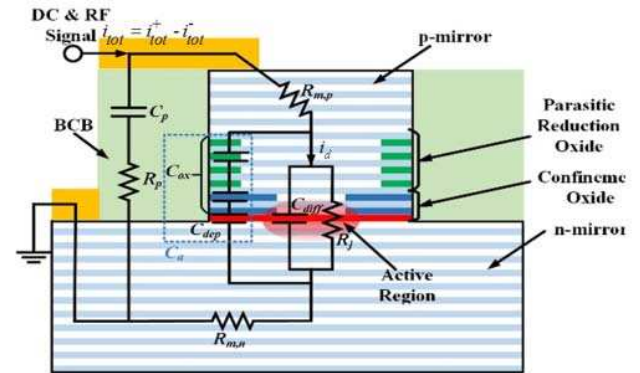


Figure 1. Physical model with equivalent circuit including the parasitic parameter identified as follows: C_p and R_p , the p-pad capacitance and resistance; $R_{m,p}$ and $R_{m,n}$, the p-DBR and n-DBR mirror series resistance; C_{diff} , diffusion capacitance at the active region; R_j , junction resistance at the active region; C_{ox} and C_{dep} , the lumped oxide capacitance and depletion capacitance. C_a is the total parasitic capacitance resulted from C_{ox} and C_{dep} .

According to two port scattering parameter, S-parameter, theory, if the mirror resistance is partially attributed to terminate the output port, the reflection coefficient, $\Gamma(f)$, is equivalent to $S_{11}(f)$ and can be expressed as

$$S_{11} = \frac{i_{tot}^-(f)}{i_{tot}^+(f)} = \frac{i_{tot}^+(f) - i_{tot}^-(f)}{i_{tot}^+(f)}, \quad (1)$$

where $i_{tot}^+(f)$ is the transmitted modulation current wave and $i_{tot}^-(f)$ is the reflected modulation current wave [7]. The total modulation current injected to the VCSEL at frequency f can be defined as $i_{tot}(f) = i_{tot}^+(f) - i_{tot}^-(f)$ at the input node. The electrical parasitic transfer function can be expressed as

$$H_{par}(f) = \frac{i_d(f)}{i_{tot}^+(f)} = \frac{i_d(f)}{i_{tot}(f)} \cdot (1 - S_{11}), \quad (2)$$

where $i_d(f)$ is the portion of the transmitted small signal modulation current that goes through the diode intrinsic active region. Hence, by fitting the $S_{11}(f)$ data with the equivalent circuit model, the electrical parasitic parameters can be extracted. Figure 2 shows the $S_{11}(f)$ data and fitting result at various biasing points for the VCSEL in the smith chart format and the extracted parameters are listed in Table I.

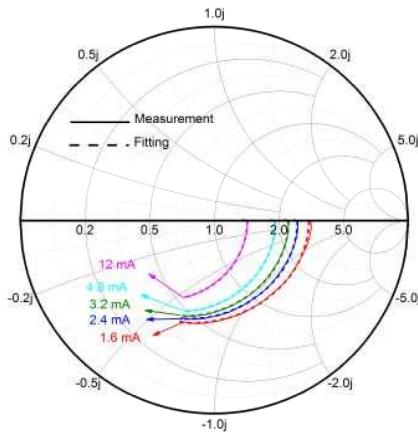


Figure 2. Measurement data and fitting of the electrical reflection coefficient of our 5 μm aperture 57 Gb/s error free VCSEL. The fitting curves are generated from the equivalent circuit shown in Fig 1. Various electrical parasitic parameters are shown in Table I.

One way to check whether the fitting result makes physical sense is to compare the mirror resistance, which is the dominant static resistance of the device, to the differential resistance derived from the I-V curve. At $I = 12$ mA, the fitted mirror resistance is 63.9 Ω and the differential resistance is 55 Ω ; the difference is about 14% and the values of the resistance are in the same order of magnitude.

OPTICAL BANDWIDTH MEASUREMENT DE-EMBEDDING

The S-parameters data, $S_{21,data}(f)$, obtained from the Agilent Parametric Network Analyzer (PNA), consists of the following superimposed microwave responses: photodetector module transfer function, $H_{PD}(f)$, laser intrinsic optical response, $S_{21,int}(f)$, and electrical parasitic transfer function, $H_{par}(f)$. The relationship of these three responses and the measurement data can be expressed as

$$dB(S_{21,data}(f)) = dB(H_{PD}(f)) + dB(S_{21,int}(f)) + dB(S_{21,par}(f)), \quad (3)$$

where the overall optical modulation response of the VCSEL is defined as

$$dB(S_{21,overall}) = dB(S_{21,int}) + dB(S_{21,par}). \quad (4)$$

In order to correctly and accurately fit the intrinsic response of the VCSEL, the photodetector and the electrical parasitic transfer function need to be de-embedded, subtracted in log scale, out of the measurement data.

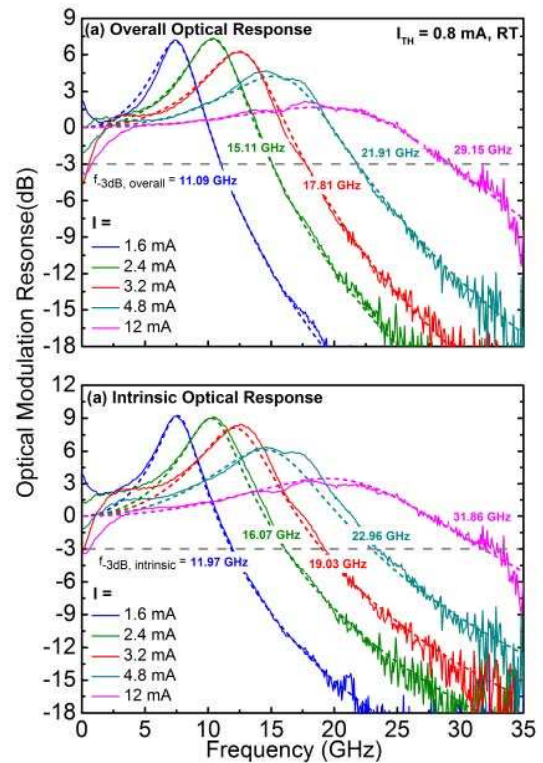


Figure 3. (a) The overall optical frequency response and (b) the intrinsic optical response of the modeled 5 μm aperture. The highest - 3dB modulation bandwidth of the overall optical response is 29.15 GHz whereas it is 31.86 GHz for the intrinsic optical response.

Table I. Fitted parasitic parameters at various biasing current points and the de-embedded intrinsic optical modulation bandwidth

d_o (μm)	I (mA)	C_p (fF)	R_p (Ω)	$R_{m,n} + R_{m,p}$ (Ω)	dV/dI (Ω)	C_a (fF)	C_{diff} (fF)	R_i (Ω)	$f_{3dB, overall}$ (GHz)	$f_{3dB, intrinsic}$ (GHz)
5	1.6	106	11.3	111	129	98	332.57	34	11.09	11.97
	2.4	103	11.1	99	111	98	372	26	15.11	16.07
	3.2	102	11	92	95	98	422	20	17.81	19.03
	4.8	97	11.1	83.5	80	98	512	12.3	21.91	22.96
	12	88	10.6	63.9	55	98	812	6.5	29.15	31.86

The photodetector transfer function is provided by the vendor, New Focus, and the electrical parasitic parameters transfer function is extracted from the equivalent circuit modeling at different biasing conditions. Hence with the photodetector and electrical parasitic parameters transfer function de-embedded, $S_{21, int}(f)$ can be fitted with the solution, shown in Eq. (1), solved from Statz and deMars rate equation [9]:

$$S_{21, int}(f) = \frac{A}{1 - f^2/f_R^2 + j(f/2\pi f_R^2)\gamma}, \quad (5)$$

where A is magnitude fitting parameter, f_R is the resonance frequency and γ is the damping rate of the optical frequency response. Figure 3 shows the overall and intrinsic optical response of the modeled VCSEL at various biasing points. At I = 12 mA, the highest extracted intrinsic -3 dB modulation bandwidth for this VCSEL is 31.8 GHz whereas the overall measured -3 dB modulation bandwidth is 29.2 GHz for this VCSEL epitaxy. The higher intrinsic optical bandwidth can be attributed to reduction of damping limitation imposed by the electrical parasitic transfer function. In the next section, the relationship between the resonance frequency and the damping rate will be examined and used to extract photon and recombination lifetime of the modeled VCSEL.

PHOTON AND RECOMBINATION LIFETIME EXTRACTION

Upon fitting the intrinsic optical response, values of the resonance frequency, f_R , and the damping rate, γ , are obtained empirically [7]. For a given VCSEL, the higher the resonance frequency, the higher the -3 dB modulation bandwidth is. Resonance frequency for VCSELs at biasing current above laser threshold current, I_{TH} , can be closely approximated as

$$f_R \approx \frac{1}{2\pi} \sqrt{\frac{v_g g' N_p}{\tau_p}} = \frac{1}{2\pi} \sqrt{\frac{v_g g'}{q V_p} \eta_i (I - I_{TH})}, \quad (6)$$

where v_g is the group velocity of the photons, g' is the differential gain, N_p is the photon density in the cavity, τ_p is the photon lifetime, V_p is the optical modal volume and η_i is the injection efficiency. It has been demonstrated that the resonance frequency can be enhanced by decreasing the photon lifetime and increasing the photon density, or output power [10]. By plotting f_R against $\sqrt{I - I_{TH}}$, the D-factor of the VCSEL can be extracted and is shown in Figure 4 (a). At high biasing current, damping rate of the

optical response is one of the factors that limit the increase of the resonance frequency and hence the modulation bandwidth. The relationship between damping rate and resonance frequency can be expressed as

$$\gamma = K f_R^2 + \frac{1}{\tau_{rec}} \approx 4\pi^2 \tau_p f_R^2 + \frac{1}{\tau_{rec}}. \quad (7)$$

The K-factor, K, relates the damping rate to the resonance frequency. By plotting the microwave modelling of γ against f_R^2 , the photon lifetime, τ_p , and recombination lifetime, τ_{rec} , can be extracted. Figure 4 (b) shows that the K-factor, and the photon lifetime, of the VCSEL can be determined from the slope of the plot and the recombination lifetime can be determined from intercept. The extracted recombination and photon lifetime are $\tau_{rec} = 0.169$ ns and $\tau_p = 4.2$ ps.

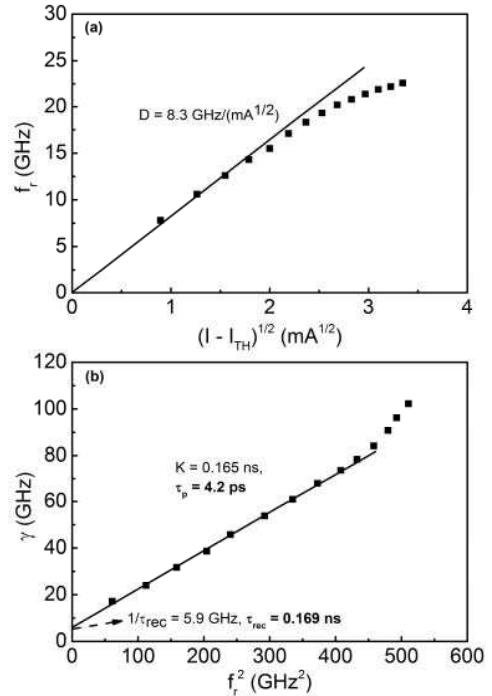


Figure 4. (a) Resonance frequency vs. $\sqrt{I - I_{TH}}$ graph. The fitted slope of the data points is the D-factor. (b) Damping rate vs. resonance frequency graph for different biasing points. The extracted photon lifetime, from the inverse of the slope, is 4.2 ps and the extracted recombination lifetime, from the intercept, is 0.169 ns.

CONCLUSION

In conclusion, we have demonstrated the microwave equivalent circuit modeling technique used to de-embed the electrical parasitic transfer function and obtain the intrinsic optical response on our 5 μm high speed oxide-confined VCSEL. The highest extracted intrinsic modulation bandwidth is 31.86 GHz. With the same technique, we have also illustrated a method to empirically extract the recombination and photon lifetime of the modeled VCSEL. The extracted $\tau_{rec} = 0.169$ ns and $\tau_p = 4.2$ ps.

ACKNOWLEDGEMENTS

This work was supported in part by the Army Research Office (Dr. Michael Gerhold) under Grant W911NF-12-1-0394 and W911NF-13-1-0287 as well as Air Force Office of Scientific Research (Dr. Kenneth Goretta) under Grant FA9550-15-1-0122. The work of N. Holonyak was supported by the Sony Corporation under the John Bardeen Endowed Chairmanship of Electrical and Computer Engineering and Physics. The work of M. Feng was supported by the Nick Holonyak, Jr. Chair of Electrical and Computer Engineering. Mr. Curtis Wang would like thank Department of Defense (DoD) for the support from the NDSEG fellowship.

REFERENCES

- [1] J. M. Dallesasse and N. Holonyak, Jr., "Native-oxide stripe-geometry Al_xGa_{1-x}As-GaAs quantum well heterostructure lasers," *Appl. Phys. Lett.*, vol. 58, no. 4, pp. 394-396, Jan. 1991
- [2] D. L. Huffaker, D. G. Deppe, K. Kumar, and T. J. Rogers, "Native-oxide defined ring contact for low threshold vertical-cavity lasers," *Appl. Phys. Lett.*, vol. 65, no. 1, pp. 97-99, Jul. 1994.
- [3] P. Westbergh, E. P. Haglund, E. Haglund, R. Safaisini, J. S. Gustavsson, and A. Larsson, "High-speed 850 nm VCSELs operating error free up to 57 Gbit/s," *Electro. Lett.*, vol.49, no.16, pp. 1021-1023, Aug. 2013.
- [4] P. Wolf, P. Moser, G. Larisch, H. Li, J. A. Lott, and D. Bimberg, "Energy efficient 40 Gbit/s transmission with 850 nm VCSELs at 108 fJ/bit dissipated heat," *Electron. Lett.*, vol. 49, no. 10, pp. 666-667, May 2013.
- [5] F. Tan, M.K. Wu, M. Liu, M. Feng, N. Holonyak, Jr., "850 nm Oxide-VCSEL with Low Relative Intensity Noise and 40 Gb/s Error Free Data Transmission," *IEEE Photon. Technol. Lett.*, vol. 26, no. 3, pp.289-292, Feb. 2014.
- [6] M. Liu, C. Y. Wang, M. Feng, and N. Holonyak, Jr. "Advanced Development of 850 nm Oxide-Confined VCSELs with 57 Gb/s Error-Free Data Transmission," in *Proc. GOMACTech*, Mar. 2016.
- [7] C. H. Wu, F. Tan, M. K. Wu, M. Feng, and N. Holonyak, Jr., "The Effect of Microcavity Laser Recombination Lifetime on Microwave Bandwidth and Eye-Diagram Signal Integrity." *J. Appl. Phys.*, vol. 109, no. 5, pp. 053112-1-053112-9, Mar. 2011.
- [8] Y. Ou, J. S. Gustavsson, P. Westbergh, Å. Haglund, A. Larsson, and A. Joel, "Impedance Characteristics and Parasitic Speed Limitations of High-Speed 850-nm VCSELs." *IEEE Photon. Technol. Lett.*, vol. 21, no. 24, pp.1840-1842, December. 2009.
- [9] H. Statz and G. deMars, *Quantum Electronics* (Columbia University Press, New York, N. Y., 1960), p. 650.
- [10] P. Westbergh, J. S. Gustavsson, B. Kögel, Å. Haglund, and A. Larsson, "Impact of Photon Lifetime on High-Speed VCSEL Performance." *IEEE J. Sel. Topics Quantum Electron.*, vol. 17, no. 6, pp. 1603-1613, Mar. 2011.

ACRONYMS

BER: Bit Error Ratio

VCSEL: Vertical Cavity Surface Emitting Laser